Organic & Biomolecular Chemistry

ROYAL SOCIETY OF CHEMISTRY

PAPER

View Article Online
View Journal | View Issue

Cite this: *Org. Biomol. Chem.*, 2025, **23**, 5805

Systematic investigation of the structure–property relationship of substituted *p*-alkoxy-azothiophenes†

Conrad Averdunk[a,b] and Hermann A. Wegner *[a,b]

Differently substituted *p*-alkoxy azothiophenes with increasing alkoxy chains were systematically investigated in terms of their structure–property relationships. In particular, it was observed that increasing the length of the alkoxy chain had an unusual effect on the melting point, which did not follow the expected odd–even effect. It was also shown that changing the length of the alkoxy chain did not significantly affect the thermal half-life, a finding that disagrees with results reported in other studies. These observations provide valuable insights into structure–property relationships with important implications for the design and development of azobenzenes as molecular materials for various applications. Furthermore, each *p*-alkoxy azothiophene was investigated in terms of neat solid-state photoisomerisation or photo-induced liquefaction, which is a critical parameter for application as a molecular solar thermal phase-change (MOST-PCM) energy storage system.

Received 26th March 2025,
Accepted 12th May 2025

DOI: 10.1039/d5ob00506j

rsc.li/obc

Introduction

Azobenzenes (ABs) are well-known photoswitches that can reversibly be switched with light irradiation between their thermodynamically stable (*E*)-isomer and the energetically excited (*Z*)-isomer.[1] Due to their photochromism, ABs have a wide range of potential applications, including as a dye,[2] in photopharmacology,[3] as a molecular wind-up meter[4] or energy storage systems.[5] In recent years, there has been growing interest in heteroaryl-substituted ABs due to their unique properties.[6] Thiophenylazobenzenes (TphABs) represent particularly interesting examples of heteroaryl-substituted ABs (Fig. 1).[7] On the one hand, the (*E*)-isomers of TphABs exhibit a significantly red-shifted absorption band of the π–π* transition, which can range from 365 nm to 405 nm depending on the substitution. On the other hand, TphABs show an almost quantitative (*E*) → (*Z*) photoisomerization, which is promoted by a strong separation of the π–π* transitions of the (*E*)- and (*Z*)-isomers. Furthermore, due to this band separation and the comparable high quantum yields of up to 44%, the photochemical back-isomerization of the (*Z*)-isomer is remarkably efficient. Additionally, the (*Z*)-isomers of TphABs show a T-shaped structure, in which the phenyl ring is orthogonal to the thiophene ring and the azo bond realizing a stabilizing intramolecular interaction between the lone pair of the sulphur atom and the π-system of the phenyl ring. This lone pair···π interaction only occurs in the (*Z*)-isomer and allows tuning of the thermal stability. Electron-withdrawing substituents on the phenyl ring can enhance the electron-donating interaction of the sulphur lone pair with the π-system, increasing the half-life of the (*Z*)-isomer.[8] Due to these different properties compared to pristine azobenzenes, the investigation of the structure–property relationship is essential for the development and optimization of heterocyclic azobenzenes as molecular materials. One potential application is the usage of azobenzenes as molecular solar thermal energy storage (MOST) systems, as alternative renewable and low-emission energy harvesting and storage systems. Such MOST systems utilize the energy difference between a higher energy meta-stable state and the ground state.[9] The class of TphABs represents a promising candidate for this application.[10] Although ABs have in general lower energy densities than the norbornadiene-quadricyclane (NBD-QC) system,[11] they excel due to their good syn-

[a]*Institute of Organic Chemistry, Justus Liebig University Giessen, Heinrich-Buff-Ring 17, 35392 Giessen, Germany.*
E-mail: Hermann.A.Wegner@org.chemie.uni-giessen.de
[b]*Center of Materials Research (ZfM/LaMa), Justus Liebig University Giessen, Heinrich-Buff-Ring 16, 35392 Giessen, Germany*

† Electronic supplementary information (ESI) available. CCDC 2425327, 2425326, 2425324 and 2425325. For ESI and crystallographic data in CIF or other electronic format see DOI: https://doi.org/10.1039/d5ob00506j

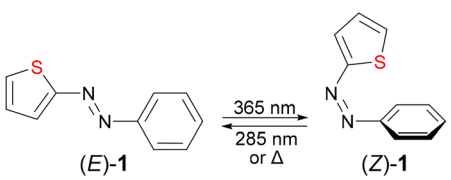

Fig. 1 Photoisomerization of TphAB **1** between (*E*)- and (*Z*)-isomers.

thetic accessibility and chemical stability compared to other photoswitches. These properties make them more suitable for commercial utilisation.[12] In recent years, a number of attempts have been made to increase the energy density.[13]

One promising approach is the combination of photoswitches with the concept of phase change materials (PCM). ABs are particularly well suited for this application because their photoisomers exhibit a significant change in geometry during photoisomerization compared to other photoswitches, leading to substantial differences in physical properties such as melting point.[14] However, the photoisomerization of crystalline ABs is challenging and has long been considered unfeasible, since crystalline structures usually provide insufficient free pore volume for molecular movement, necessary for photoisomerization.[15] In recent years, however, several AB-based MOST-PCM systems have been developed in which photoisomerization and liquefaction of crystalline ABs upon irradiation were achieved.[16] In these systems, the ABs are typically equipped with at least one alkyl chain. Systems with additional substituents are also known.[17–19] Several azopyrazole- and azoisoxazole-based systems have also been reported that can be used as MOST-PCM systems.[20,21] The combination of heterocyclic ABs with MOST-PCM systems is particularly interesting for tuning the properties of such systems.

For this reason, TphABs with different alkoxy chains at the *para*-position of the phenyl moiety were synthesised in this study. The *para*-substitution was chosen because almost all literature known MOST-PCM systems are *para*-substituted although we have shown that *meta*-substitution would significantly prolong the thermal half-life.[8] Furthermore, substitution in the *para*-position enables much better synthetic accessibility. In addition, the substituent on the thiophene ring was varied. A methyl and a methoxy group were used to investigate the influence of a second substituent on the physicochemical properties. The methoxy group was chosen to study whether introducing a second, free rotating substituent could have a positive effect on molecular mobility within the crystal structure and enhance photoliquefaction. The shorter, more rigid methyl group was used as a reference. In this study melting points, kinetic half-lives, crystal structures, absorption spectra and solid-state photoisomerization were investigated to establish the valuable structure–property relationship which will contribute to the development of new MOST-PCM systems.

Results and discussion

Synthesis

First, 4-alkoxyphenyl-5-methoxythiophenyldiazenes (**4a–i**) were successfully synthesised by a two-step synthesis involving an azo-coupling reaction followed by Williamson etherification (Fig. 2a). Therefore, 4-aminophenol (**2**) was converted to a diazonium salt and treated with the electron-rich 2-methoxythiophene under basic conditions to obtain the hydroxy substituted methoxy TphAB **3** *via* an azo-coupling reaction.[22] The electron-donating effect of the methoxy group at the C5 position of the thiophene increases the acidity of the proton providing good nucleophilicity. The resulting TphAB **3** was then etherified to obtain the desired TphABs **4a–i**. Due to the insufficient electron density of the methyl substituted thiophene, a slightly different method was applied for the synthesis of TphABs **9a–e** (Fig. 2b). In these cases, the corresponding bromides were used and first converted to the corresponding Grignard reagents.[23] These intermediates were then treated with zinc bromide to obtain the corresponding organozinc compounds to obtain a suitable nucleophile, which undergoes efficient azo-coupling reactions under mild con-

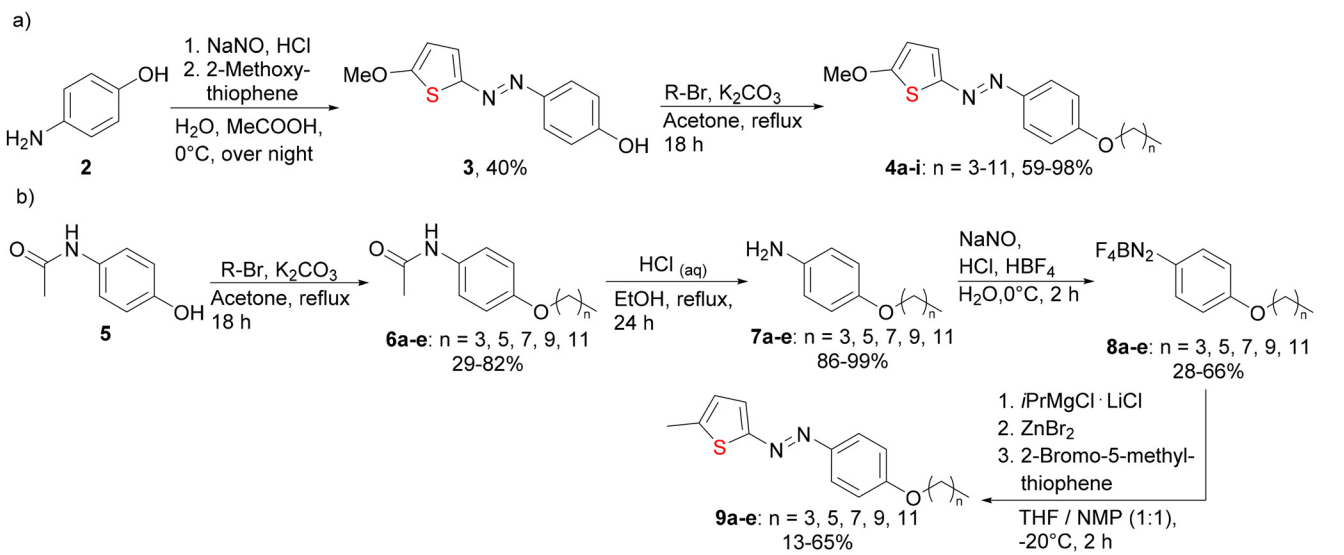

Fig. 2 (a) Synthesis of 4-alkoxyphenyl-5-methoxythiophenyldiazenes **4a–i** *via* an azo-coupling reaction followed by Williamson etherification. (b) Synthesis of 4-alkoxyphenyl-5-methylthiophenyldiazenes **9a–e** *via* an azo-coupling reaction with diazonium salts **8a–e** and zinc organyl.

ditions with the corresponding diazonium salts **8a–e** to provide the TphABs **9a–e**.[24]

Melting points

A deep understanding of the structure–property relationship is essential for the development and optimisation of new molecular materials. One of the most important parameters in this context is the melting point of the (*E*)- and (*Z*)-isomers, as it determines the temperature range in which the system can be operated. The melting point of the isomers is also a critical factor in the success and efficiency of photoliquefaction, as excessively high melting points, particularly of the (*E*)-isomer, can make the irradiation induced liquefaction process less advantageous. In such cases, a larger temperature difference may need to be compensated by a higher proportion of the (*Z*)-isomer. In this study, the melting points of the respective (*E*)-isomers of different TphABs were determined in order to gain insights into the relationship between melting points, chain length and substituents (Fig. 3). The (*E*)-isomers of the methoxy-substituted TphABs **4a–i** revealed an increase in melting point with increasing chain length, which can be attributed to the increasing intermolecular interactions between the alkoxy chains (Fig. 3; red dots). A commonly observed phenomenon in compounds with long alkyl chains is the so-called odd–even effect, where stronger interactions between the chains occur in compounds with an even number chain length compared to those with an odd number chain length.[25] In general, it can be assumed that compounds with an even number of carbon atoms in their chains tend to have slightly higher melting points than those with an odd number of carbon atoms.[26] Here, an unusual trend in the melting points as a function of chain length was observed. Specifically, a significant decrease in melting point occurred for every third additional carbon of the alkoxy chain, while the remaining chain lengths followed a relatively linear behaviour.

It seemed that the melting points of TphABs **4a–i** follow two distinct trends. In particular, TphABs **4a–i** with chain lengths of C4, C7 and C10 showed significantly lower melting points. In contrast, the methyl-substituted TphABs neither showed a comparable trend nor any linear or increasing behaviour of the melting points with increasing chain length. With the more rigid molecular geometry, a rather linear behaviour of the melting point could be expected. As only alkoxy groups with an even chain length were investigated for the methyl-substituted TphABs, no conclusions can be made concerning the influence of the odd–even effect. This shows that in general there is no trivial linear relationship between chain length and melting point. This is in accordance with literature known MOST-PCM systems, where also no correlation of the melting point with increasing chain length has been observed so far.[17,19,21]

Spectroscopic properties

The methyl and methoxy substituted TphABs **4a–i** and TphABs **9a–e** were dissolved in acetonitrile and irradiated at different wavelengths to determine the wavelength for the most effective photoisomerization (Fig. 4). The absorption spectrum of the initial state of the TphABs **4** shows a strong absorption band around 400 nm corresponding to the π–π* transition and a shoulder around 450 nm corresponding to the n–π* transition (Fig. 4, red). Irradiation with a wavelength of 405 nm leads to a significant decrease in the intensity of the π–π* band and the appearance of a new band around 330 nm. Different wavelengths were tested to determine the most efficient (*Z*) → (*E*) isomerization. It was found that a wavelength of 265 nm resulted in almost quantitative back-isomerization. Compared to the methoxy substituted TphABs **4a–i**, the methyl substituted TphABs **9a–e** show a less red-shifted absorption maximum of the π–π* transition band at approx. 385 nm. Back switching was also carried out with a wavelength of 265 nm. This process was not as effective as for the methoxy substituted TphABs **4a–i**. However, it was not possible to accurately determine the composition of the (*E*)- and (*Z*)-isomers in the

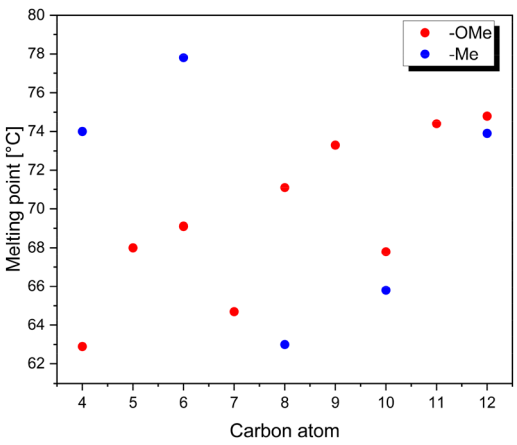

Fig. 3 Melting points of the (*E*)-isomers of methyl and methoxy substituted TphABs **4a–i** and TphABs **9a–e** with different chain lengths.

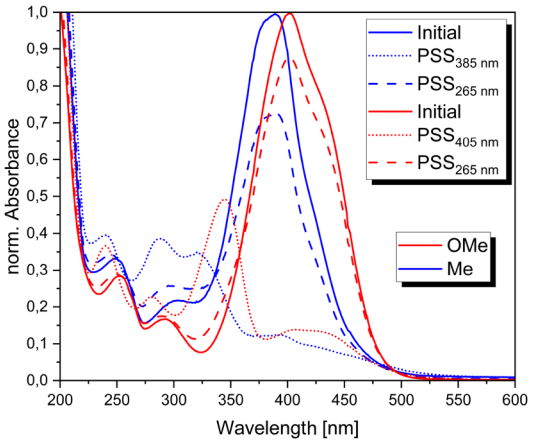

Fig. 4 UV-Vis absorption spectra of the initial state and photostationary states (PSS) at different wavelengths for photoisomerization from the (*E*)- to (*Z*)-isomer and back-switching in ACN of methyl and methoxy substituted TphAB **4g** and TphAB **9d**.

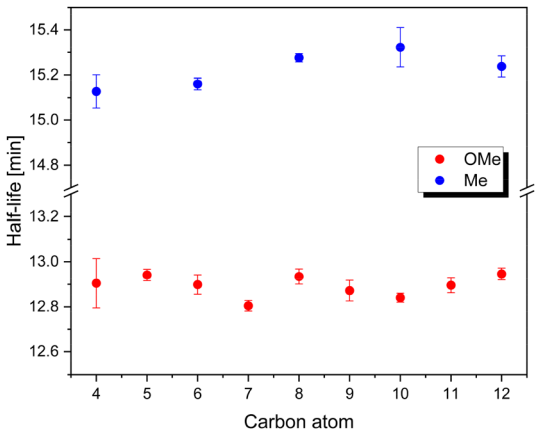

Fig. 5 Thermal half-lives of methoxy and methyl substituted TphABs **4a–i** and TphABs **9a–e** at 20 °C in acetonitrile.

photostationary state at the different wavelengths, as the thermal half-lives of the TphABs **4a–i** and **9a–e** in solution are too short to determine their composition by NMR spectroscopy or HPLC (Fig. 5).

Thermal isomerization kinetics

The thermal half-lives of methoxy and methyl substituted TphABs **4a–i** and TphABs **9a–e** have been determined using UV-Vis spectroscopy. The methoxy-substituted TphABs **4a–i** showed an average thermal half-life of just under 13 min. In comparison, the methyl-substituted TphABs **9a–e** showed a slightly longer thermal half-life of just over 15 min on average. This drastically reduced half-life can be explained by electronic effects. Due to the electron-donating effect of the alkoxy group on the phenyl ring, the electron density is increased, which reduces the electron-donating intramolecular Lp···π interaction between the lone pair of the sulphur atom and the π system of the phenyl ring. This effect leads to less stabilization of the (*Z*)-isomer, resulting in a significant decrease in its thermal half-life. Similar observations have been made in comparable TphAB systems.[8] Furthermore, the thermal half-life is not affected by chain length, which is in contrast to analogous literature-known systems.[27]

Photoliquefaction properties

All synthesised TphABs were irradiated in the solid state at different wavelengths and temperatures to investigate their potential as candidates for MOST-PCM materials. It was found that the methoxy-substituted TphABs **4a–i** do not show any photoliquefaction upon irradiation with 405 nm, which corresponds to the absorption maximum of the π–π* transition of the (*E*)-isomer in solution. The same observation was made for the methyl-substituted TphABs **9a–e** upon irradiation with 385 nm, which could be caused by a significant shift of the π–π* transition band in the solid state compared to that in solution, preventing effective excitation with 405 nm or 385 nm. In other MOST-PCM systems, a strong redshift of the π–π* transition has been observed in the solid state, with a shift in excitation in solution from around 340 nm to around 365 nm in the solid state.[17] During irradiation a colour change

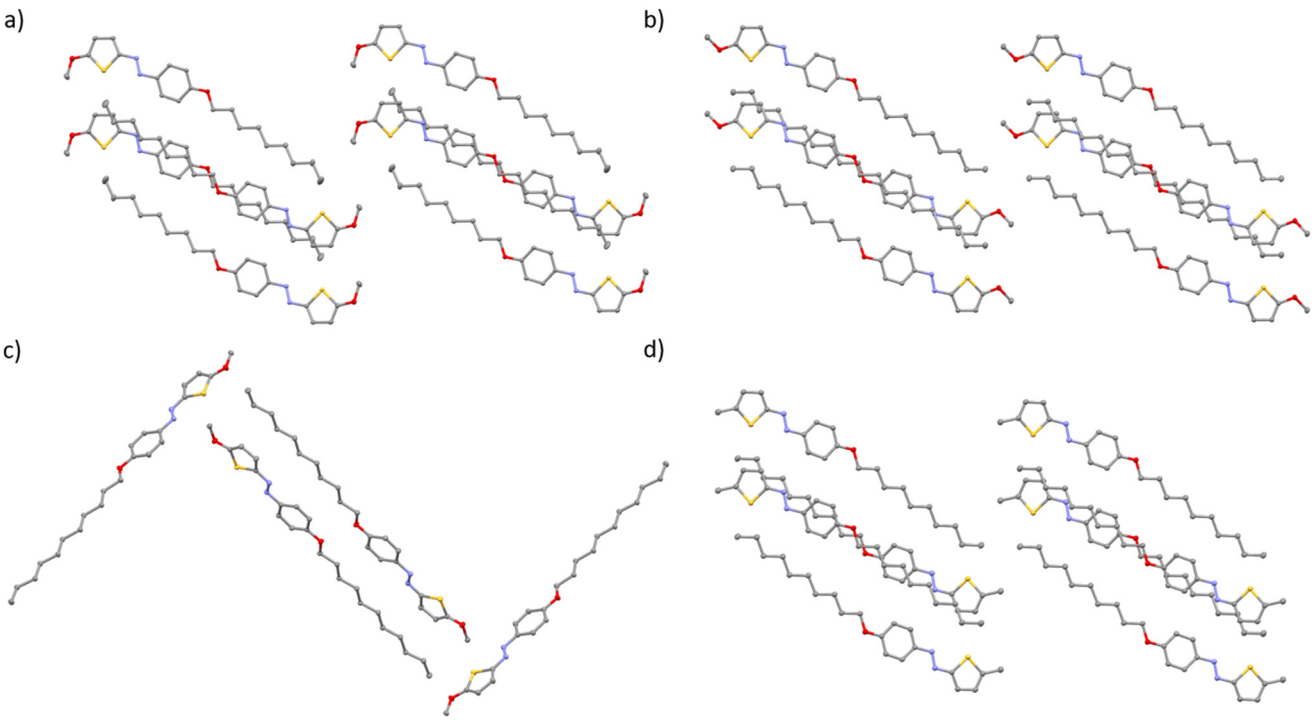

Fig. 6 Crystal structures of (*E*)-4-alkoxyphenyl-5-methoxythiophenyldiazenes with (a) C9, (b) C10 and (c) C11 chain lengths and (d) (*E*)-4-alkoxyphenyl-5-methylthiophenyldiazene with C10 chain length.

was observed indicating possible photoisomerization in the solid state. Therefore, a potential reason for unsuccessful photoliquefaction could be the high melting points of the (*E*)- and (*Z*)-isomers, which may prevent effective liquefaction of the solid phase upon irradiation. To promote photoliquefaction, the respective compounds were heated during irradiation to temperatures just below the melting point of the (*E*)-isomer. However, these conditions also did not lead to a successful photoliquefaction. In this case it is also important to consider the short half-lives, which are further reduced by the additional heating, potentially making effective photoisomerization more challenging. The most likely cause of unsuccessful photoliquefaction is an insufficient mobility of the molecules within the crystal structure, which suppresses and prevents photoisomerization in the solid phase. In addition, NMR-spectroscopy revealed decomposition after prolonged irradiation, which may also cause colour change.

Solid state structures

The solid-state structures of methoxy-substituted TphABs **4f–h** with chain lengths of C9, C10 and C11 and that of methyl substituted TphAB **9d** were obtained (Fig. 6). A comparison of the crystal structures of the C9 (Fig. 6a) and C10 (Fig. 6b) derivatives showed that they have similar crystal packing. The only difference, apart from the chain length, is the orientation of the methoxy group. For the TphAB **4f** with a C9 chain, the methoxy group is in the plane of the thiophene ring and faces the sulphur atom, whereas for the TphAB **4f** with a C10 chain it is oriented in the opposite direction. Thus, the orientation of the methoxy group could potentially explain the unusual decrease of melting point. Compound **4h** adopts a completely different packing, which makes it only partially comparable with the crystal structures of TphABs **4f** and **g**. In the solid-state structure of **4h** we also find that here the methoxy group points in the opposite direction to the sulphur atom.

The methyl substituted TphAB **9d** shows a similar packing to the methoxy substituted TphABs **4f** and **g** indicating that the alkoxy group mainly determines the crystal packing. Since the methyl substituent in TphABs **9a–e** is fixed and cannot change its orientation it could be assumed that the melting points should show a more linear behaviour with increasing chain length. In summary, no clear correlation between melting points and any structural properties could be assigned.

Conclusions

Various substituted TphABs with different substituents and chain lengths were successfully synthesised and their physical properties were investigated. It was shown that methoxy and methyl substituted TphABs **4a–i** and TphABs **9a–e** show promising properties for lower energy absorption, as they exhibit a significant red shift of the π–π* transition reaching up to 405 nm. It was shown that there is no correlation between chain length and thermal half-life in solution for the synthesised TphABs. An unusual trend in the melting points as a function of chain length was also observed for the methoxy substituted TphABs **9a–e**, with a significant decrease in melting point for every third additional carbon in the alkoxy chain. This behaviour is contrary to other MOST-PCM systems and the textbook-known odd–even effect.[28] In addition, single crystals were obtained which allowed a more detailed analysis of the structural effects in the solid state *via* X-ray analysis. For the methyl substituted TphABs **9a–d** no correlation of the melting point or the chain length was observed, though. Photoliquefaction could not be achieved for any of the TphABs by irradiation with different wavelengths and temperatures. This behaviour might be due to reduced molecular mobility in the solid state, the high melting points of the (*E*)-isomers, short thermal half-lives as well as decomposition. To realize the concept of MOST-PCM systems with azothiophenes, it is necessary to increase the thermal half-life to achieve sufficient photoisomerization in the condensed phase. Furthermore, it is essential to prevent irradiation-induced decomposition by selective substitution of the thiophene moiety. Additionally, an increase of the free pore volume and a reduction of the melting points of the (*E*)-isomers could enhance photoliquefaction. For example, the substitution of the alkoxy chain in the *meta*-position could not only offer an increased thermal half-life but could also adapt the melting point and the free pore volume due to the lower symmetry. Nevertheless, valuable information has been gained, which supports the design of novel molecular materials with application potential as MOST-PCMs in the future.

Author contributions

H. A. W. and C. A. conceptualized the project and prepared the manuscript. C. A. synthesized all compounds and collected all experimental data. Both authors were involved in discussing the data and have given approval to the final version of the manuscript.

Data availability

The data supporting this article have been included as part of the ESI.†

Conflicts of interest

There are no conflicts to declare.

Acknowledgements

The authors acknowledge the financial support from the Deutsche Forschungsgemeinschaft (DFG) within the Research Unit FOR 5499 "Molecular Solar Energy Management – Chemistry of MOST Systems" (project 496207555). We thank

Dominic Schatz, Institute of Organic Chemistry of the Justus Liebig University, for X-ray analysis.

References

1 A. A. Beharry and G. A. Woolley, *Chem. Soc. Rev.*, 2011, **40**, 4422–4437.
2 A. Bafana, S. S. Devi and T. Chakrabarti, *Environ. Rev.*, 2011, **19**, 350–371.
3 V. A. Gutzeit, A. Acosta-Ruiz, H. Munguba, S. Häfner, A. Landra-Willm, B. Mathes, J. Mony, D. Yarotski, K. Börjesson, C. Liston, G. Sandoz, J. Levitz and J. Broichhagen, *Cell Chem. Biol.*, 2021, **28**, 1648–1663.
4 C. Averdunk, K. Hanke, D. Schatz and H. A. Wegner, *Acc. Chem. Res.*, 2024, **57**, 257–266.
5 (*a*) E. N. Cho, D. Zhitomirsky, G. G. D. Han, Y. Liu and J. C. Grossman, *ACS Appl. Mater. Interfaces*, 2017, **9**, 8679–8687; (*b*) J. Huang, Y. Jiang, J. Wang, C. Li and W. Luo, *Thermochim. Acta*, 2017, **657**, 163–169; (*c*) A. M. Kolpak and J. C. Grossman, *Nano Lett.*, 2011, **11**, 3156–3162; (*d*) A. M. Kolpak and J. C. Grossman, *J. Chem. Phys.*, 2013, **138**, 34303; (*e*) W. Pang, J. Xue and H. Pang, *Sci. Rep.*, 2019, **9**, 5224; (*f*) B. Zhang, Y. Feng and W. Feng, *Nano Lett.*, 2022, **14**, 138.
6 S. Crespi, N. A. Simeth and B. König, *Nat. Rev. Chem.*, 2019, **3**, 133–146.
7 C. Slavov, C. Yang, A. H. Heindl, H. A. Wegner, A. Dreuw and J. Wachtveitl, *Angew. Chem., Int. Ed.*, 2020, **59**, 380–387.
8 A. H. Heindl and H. A. Wegner, *Chemistry*, 2020, **26**, 13730–13737.
9 Z. Wang, P. Erhart, T. Li, Z.-Y. Zhang, D. Sampedro, Z. Hu, H. A. Wegner, O. Brummel, J. Libuda, M. B. Nielsen and K. Moth-Poulsen, *Joule*, 2021, **5**, 3116–3136.
10 E. Franz, A. Kunz, N. Oberhof, A. H. Heindl, M. Bertram, L. Fusek, N. Taccardi, P. Wasserscheid, A. Dreuw, H. A. Wegner, O. Brummel and J. Libuda, *ChemSusChem*, 2022, **15**, e202200958.
11 (*a*) F. Hemauer, H.-P. Steinrück and C. Papp, *ChemPhysChem*, 2024, **25**, e202300806; (*b*) M. J. Kuisma, A. M. Lundin, K. Moth-Poulsen, P. Hyldgaard and P. Erhart, *J. Phys. Chem. C*, 2016, **120**, 3635–3645; (*c*) J. Orrego-Hernández, A. Dreos and K. Moth-Poulsen, *Acc. Chem. Res.*, 2020, **53**, 1478–1487; (*d*) A. U. Petersen, A. I. Hofmann, M. Fillols, M. Mansø, M. Jevric, Z. Wang, C. J. Sumby, C. Müller and K. Moth-Poulsen, *Adv. Sci.*, 2019, **6**, 1900367; (*e*) M. Quant, A. Lennartson, A. Dreos, M. Kuisma, P. Erhart, K. Börjesson and K. Moth-Poulsen, *Chemistry*, 2016, **22**, 13265–13274; (*f*) F. Waidhas, M. Jevric, L. Fromm, M. Bertram, A. Görling, K. Moth-Poulsen, O. Brummel and J. Libuda, *Nano Energy*, 2019, **63**, 103872; (*g*) R. Schulte, S. Afflerbach, T. Paululat and H. Ihmels, *Angew. Chem., Int. Ed.*, 2023, **62**, e202309544.
12 (*a*) E. Merino, *Chem. Soc. Rev.*, 2011, **40**, 3835–3853; (*b*) C.-L. Sun, C. Wang and R. Boulatov, *ChemPhotoChem*, 2019, **3**, 268–283.
13 (*a*) X. Xu, J. Feng, W.-Y. Li, G. Wang, W. Feng and H. Yu, *Prog. Polym. Sci.*, 2024, **149**, 101782; (*b*) A. Kunz, A. H. Heindl, A. Dreos, Z. Wang, K. Moth-Poulsen, J. Becker and H. A. Wegner, *ChemPlusChem*, 2019, **84**, 1145–1148; (*c*) A. R. Ibrahim, M. F. Khyasudeen, J. Husband, S. M. Alauddin, N. F. K. Aripin, T. S. Velayutham, A. Martinez-Felipe and O. K. Abou-Zied, *J. Phys. Chem. C*, 2021, **125**, 22472–22482; (*d*) Z. Wang, R. Losantos, D. Sampedro, M.-A. Morikawa, K. Börjesson, N. Kimizuka and K. Moth-Poulsen, *J. Mater. Chem. A*, 2019, **7**, 15042–15047.
14 (*a*) G. S. Kumar and D. C. Neckers, *Chem. Rev.*, 1989, **89**, 1915–1925; (*b*) W.-C. Xu, S. Sun and S. Wu, *Angew. Chem., Int. Ed.*, 2019, **58**, 9712–9740.
15 A. Gonzalez, E. S. Kengmana, M. V. Fonseca and G. G. D. Han, *Mater. Today Adv.*, 2020, **6**, 100058.
16 (*a*) J. Ge, M. Qin, X. Zhang, X. Yang, P. Yang, H. Wang, G. Liu, X. Zhou, B. Zhang, Z. Qu, Y. Feng and W. Feng, *SmartMat*, 2024, **5**, e1300; (*b*) J. Hu, S. Huang, M. Yu and H. Yu, *Adv. Energy Mater.*, 2019, **9**, 1901363; (*c*) H. Liu, Y. Feng and W. Feng, *Compos. Commun.*, 2020, **21**, 100402; (*d*) J. Tang, Y. Feng and W. Feng, *Compos. Commun.*, 2021, **23**, 100575.
17 J. Gao, Y. Feng, W. Fang, H. Wang, J. Ge, X. Yang, H. Yu, M. Qin and W. Feng, *Energy Environ. Mater.*, 2024, **7**, e12607.
18 (*a*) Y. Shi, M. A. Gerkman, Q. Qiu, S. Zhang and G. G. D. Han, *J. Mater. Chem. A*, 2021, **9**, 9798–9808; (*b*) J. Hu, M. Yu and H. Yu, *J. Mater. Chem. C*, 2025, **35**, 4621.
19 Y. Yang, S. Huang, Y. Ma, J. Yi, Y. Jiang, X. Chang and Q. Li, *ACS Appl. Mater. Interfaces*, 2022, **14**, 35623–35634.
20 (*a*) A. Gonzalez, M. Odaybat, M. Le, J. L. Greenfield, A. J. P. White, X. Li, M. J. Fuchter and G. G. D. Han, *J. Am. Chem. Soc.*, 2022, **144**, 19430–19436; (*b*) X. Huang, Z. Shangguan, Z.-Y. Zhang, C. Yu, Y. He, D. Fang, W. Sun, Y.-C. Li, C. Yuan, S. Wu and T. Li, *Chem. Mater.*, 2022, **34**, 2636–2644; (*c*) Z. Shangguan, W. Sun, Z.-Y. Zhang, D. Fang, Z. Wang, S. Wu, C. Deng, X. Huang, Y. He, R. Wang, T. Li, K. Moth-Poulsen and T. Li, *Chem. Sci.*, 2022, **13**, 6950–6958; (*d*) L. Burg, L. Kortekaas, A. Gibalova, C. Daniliuc, J. Heßling, M. Schönhoff and B. J. Ravoo, *RSC Appl. Interfaces*, 2025, **2**, 373–380; (*e*) L. Kortekaas, J. Simke, D. W. Kurka and B. J. Ravoo, *ACS Appl. Mater. Interfaces*, 2020, **12**, 32054–32060.
21 Z.-Y. Zhang, Y. He, Z. Wang, J. Xu, M. Xie, P. Tao, D. Ji, K. Moth-Poulsen and T. Li, *J. Am. Chem. Soc.*, 2020, **142**, 12256–12264.
22 A. Matharu, P. Huddleston, S. Jeeva, M. Wood and D. Chambers-Asman, *Dyes Pigm.*, 2008, **78**, 89–92.
23 (*a*) A. Krasovskiy and P. Knochel, *Angew. Chem., Int. Ed.*, 2004, **43**, 3333–3336; (*b*) A. Krasovskiy and P. Knochel, *Angew. Chem.*, 2004, **116**, 3396–3399.
24 (*a*) B. Haag, Z. Peng and P. Knochel, *Org. Lett.*, 2009, **11**, 4270–4273; (*b*) D. Y. Curtin and J. A. Ursprung, *J. Org.*

Chem., 1956, **21**, 1221–1225; (*c*) D. Y. Curtin and J. L. Tveten, *J. Org. Chem.*, 1961, **26**, 1764–1768.

25 W. H. de Jeu, J. van der Veen and W. J. A. Goossens, *Solid State Commun.*, 1973, **12**, 405–407.

26 K. Yang, Z. Cai, A. Jaiswal, M. Tyagi, J. S. Moore and Y. Zhang, *Angew. Chem., Int. Ed.*, 2016, **55**, 14090–14095.

27 (*a*) Q. Qiu, M. A. Gerkman, Y. Shi and G. G. D. Han, *Chem. Commun.*, 2021, **57**, 9458–9461; (*b*) Z. Abdin, M. A. Alim, R. Saidur, M. R. Islam, W. Rashmi, S. Mekhilef and A. Wadi, *Renewable Sustainable Energy Rev.*, 2013, **26**, 837–852; (*c*) L. Jiang, Z. Wu, H. Liu, L. Zhang and X. Luo, *Appl. Mater. Today*, 2025, **42**, 102531; (*d*) Q. Yang, J. Ge, M. Qin, H. Wang, X. Yang, X. Zhou, B. Zhang, Y. Feng and W. Feng, *Sci. China Mater.*, 2023, **66**, 3609–3620; (*e*) L. Fei, Y. Yin, J. Zhang and C. Wang, *Sol. RRL*, 2020, **4**, 105; (*f*) L. Fei, W. Yu, J. Tan, Y. Yin and C. Wang, *Adv. Fiber Mater.*, 2023, **5**, 955–967.

28 J. C. S. Costa and L. M. N. B. F. Santos, *J. Chem. Eng. Data*, 2019, **64**, 2229–2246.